Spatiotemporal ITCZ dynamics during the last three millennia in Northeastern Brazil and related impacts in modern human history

Giselle Utida[1]*, Francisco W. Cruz[1], Mathias Vuille[2], Angela Ampuero[1], Valdir F. Novello[3], Jelena Maksic[4], Gilvan Sampaio[5], Hai Cheng[6,7,8], Haiwei Zhang[6]; Fabio Ramos Dias de Andrade[1], R. Lawrence Edwards[9]

[1]Instittuto de Geociências, Universidade de São Paulo, Rua do Lago, 562, Cidade Universitária, São Paulo-SP, 05508-090, Brazil

[2]Department of Atmospheric and Environmental Sciences, University at Albany, SUNY, Albany, NY, USA

[3]Geo- and Environmental Research Center, University of Tübingen, Tübingen, Germany

[4]Division of Impacts, Adaptation and Vulnerabilities (DIIAV), National Institute for Space Research (INPE), São Jose dos Campos-SP, Brazil

[5]General Coordination of Earth Science (CGCT), National Institute for Space Research (INPE), Sao Jose dos Campos-SP, Brazil

[6]Institute of Global Environmental Change, Xi'an Jiaotong University, Xi'an, China

[7]State Key Laboratory of Loess and Quaternary Geology, Institute of Earth Environment, Chinese Academy of Sciences, Xi'an, China

[8]Key Laboratory of Karst Dynamics, MLR, Institute of Karst Geology, CAGS, China

[9]Department of Earth Sciences, University of Minnesota, Minneapolis, MN, USA

*Corresponding author: giselleutida@hotmail.com

Supplementary Material

5 figures and 4 tables.

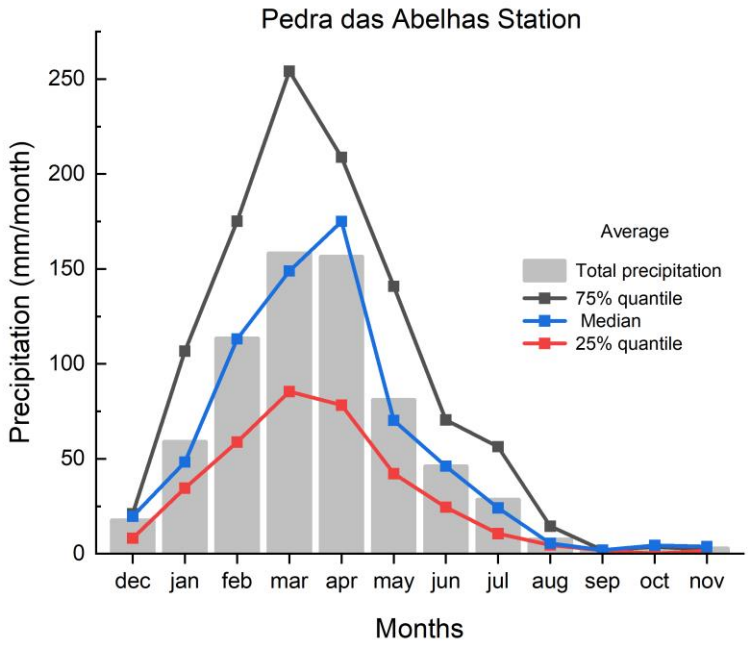

Figure S1 - Pedra das Abelhas ANA Station precipitation analyzed from 1911 to 2015 (n=103), excluding the strongest ENSO years (39 years), according to Araújo et al. (2013).

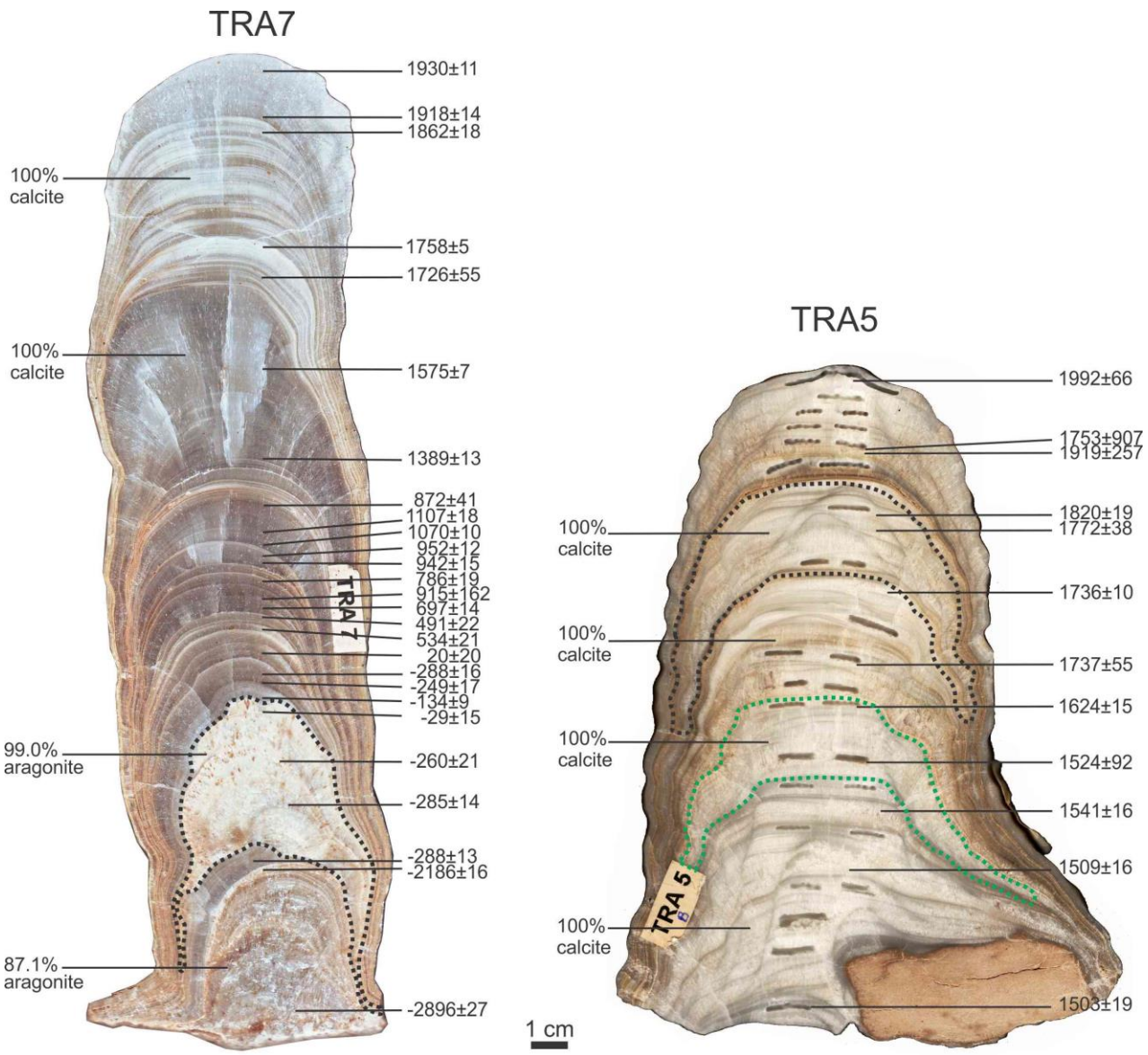

Figure S2 – TRA7 and TRA5 speleothem images indicating results of U/Th ages in BCE/CE and mineralogical composition. Outlines indicate the portions according to mineralogy. TRA7 ages and mineralogy obtained by Utida et al. (2020).

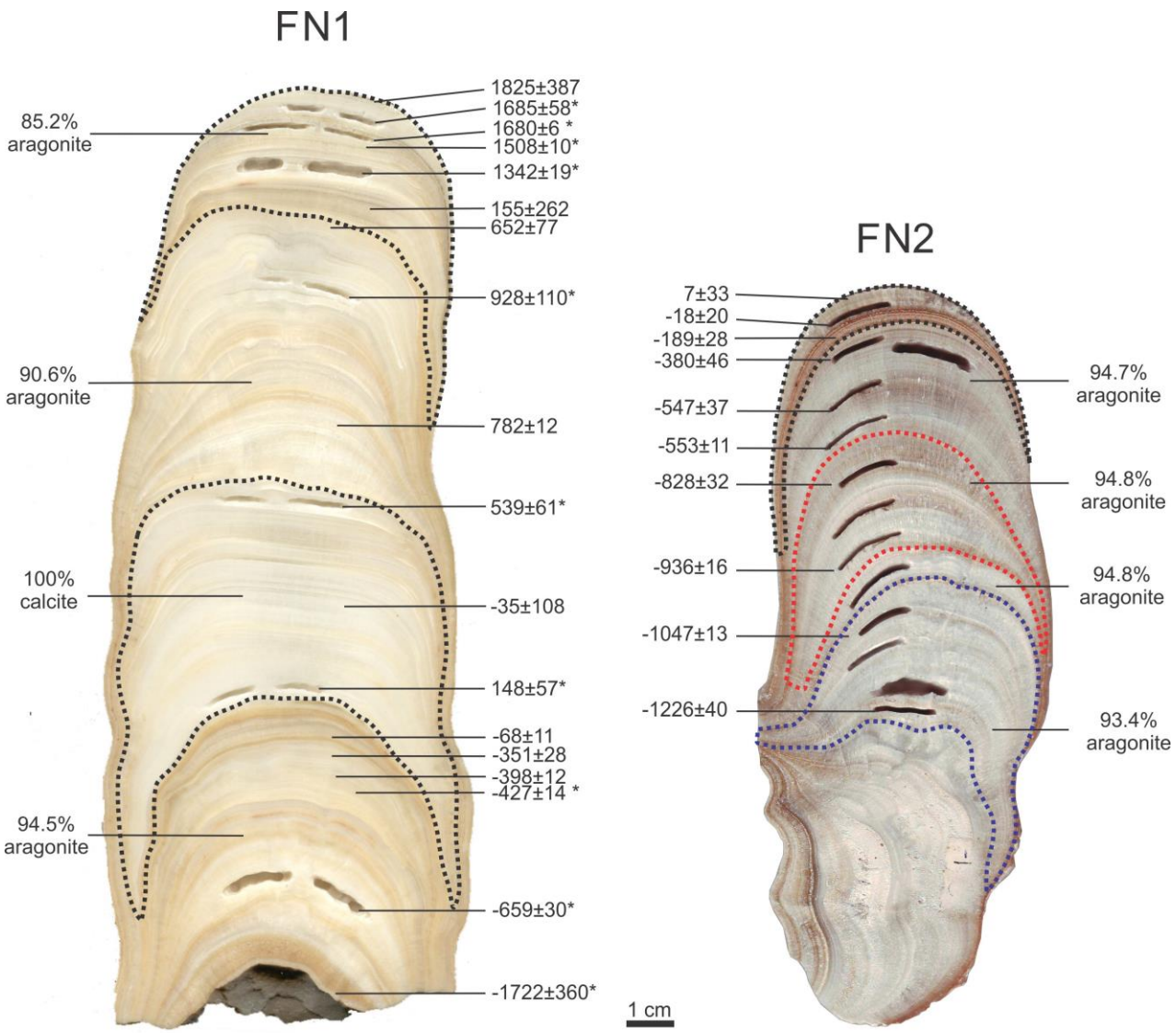

Figure S3 – Speleothem FN1 and FN2 images indicating results of U/Th ages BCE/CE. Outlines indicate the portions according to mineralogy. * FN1 ages obtained by Cruz et al. (2009). FN1 mineralogy obtained by Utida et al. (2020).

Table S1 – Chronological results. U/Th results obtained from speleothem FN1 and FN2. *Data obtained by Cruz et al. (2009).

Sample Number	Depth (mm)	^{238}U (ppb)		^{232}Th (ppt)		^{230}Th / ^{232}Th (atomic x10^{-6})		$d^{234}U$* (measured)		^{230}Th / ^{238}U (activity)		^{230}Th Age (yr) (uncorrected)		^{230}Th Age (yr) (corrected)		$d^{234}U_{Initial}$** (corrected)		^{230}Th Age (yr BP)*** (corrected)		Age BCE/CE
FN1 speleothem																				
FN1-1	**1**	214	± 1	3824.9	± 18	5.8	±2	-59.5	±4	0.0064	±0.00232	739	±271	183	±387	-60	±4	125	±387	1825
FN1-a*	**5**	119	± 0	228	± 2	28	±4	-68	±3	0,0033	±0,00043	383	±50	323	±58	-68	±3	265	±58	1685
FN1-b*	**9**	4134	± 16	698	± 2	280	±5	-58	±1	0,0029	±0,00005	333	±6	328	±6	-58	±1	270	±6	1680
FN1-B1*	**12**	7837	± 26	3878	± 10	148	±2	-58	±2	0,0044	±0,00006	515	±7	500	±10	-58	±2	442	±10	1508
FN1-T*	**16**	1152	± 4	1256	± 3	91	±1	-61	±2	0,0060	±0,00007	700	±9	666	±19	-61	±2	608	±19	1342
FN1-22	**22**	701	± 2	8378	± 169	26	±1	-58	±2	0,0191	±0,00013	2234	±17	1864	±262	-58	±2	1795	±262	155
FN1-T2	**29**	812	± 1	2425	± 49	69	±2	-56	±1	0,0125	±0,00034	1453	±40	1360	±77	-57	±1	1298	±77	652
FN1-2*	**41**	48	± 0	151	± 2	54	±5	-53	±2	0,0102	±0,00089	1180	±100	1080	±110	-53	±2	1022	±110	928
FN1-2A	**72**	5814	± 36	1171	± 6	868	±7	-57	±4	0.0106	±0,00009	1232	±12	1226	±12	-57	±4	1168	±12	782
FN1-3*	**88**	85	± 0	209	± 1	90	±3	-56	±2	0,0133	±0,00041	1545	±48	1469	±61	-56	±2	1411	±61	539
FN1-106	**106**	508	± 1	2506	± 50	63	±1	-52	±2	0,0190	±0,00014	2205	±16	2054	±108	-52	±2	1985	±108	-35
FN1-4*	**127**	75	± 0	97	± 1	210	±7	-53	±3	0,0164	±0,00046	1899	±54	1860	±57	-53	±3	1802	±57	148
FN1-4.1	**137**	13580	± 49	2593	± 53	1535	±31	-62	±2	0,0178	±0,00008	2086	±10	2080	±11	-62	±2	2018	±11	-68
FN1-140	**140**	12302	± 97	9588	± 208	433	±9	-57	±3	0,0205	±0,00017	2394	±22	2370	±28	-57	±3	2301	±28	-351
FN1-4.2	**145**	15185	± 51	4074	± 82	1271	±26	-57	±2	0,0207	±0,00008	2418	±10	2410	±12	-57	±2	2348	±12	-398
FN1-4A*	**147**	17533	± 81	3486	± 7	1734	±6	-55	±2	0,0209	±0,00011	2441	±14	2435	±14	-56	±2	2377	±14	-427
FN1-B*	**187**	20240	± 200	2847	± 8	2680	±12	-55	±3	0,0229	±0,00024	2671	±30	2667	±30	-55	±3	2609	±30	-659
FN1-4B*	**202**	7297	± 22	165820	± 830	27	±1	-52	±2	0,0377	±0,00076	4435	±91	3730	±360	-52	±2	3672	±360	-1722
FN2 speleothem																				
FN2-1	**1**	4480	± 13	7017	± 142	197	±4	-1	±2	0,0187	±0,00007	2058	±8	2012	±33	-1	±2	1943	±33	7
FN2-4	**4**	5566	± 15	4344	± 12	392	±3	-4	±2	0,0185	±0,00000	2052	±16	2030	±20	-4	±2	1968	±20	-18
FN2-6	**6**	5161	± 31	5881	± 123	294	±6	0	±3	0,0203	±0,00013	2241	±16	2208	±28	0	±3	2139	±28	-189
FN2-2	**10**	4525	± 17	9648	± 196	172	±4	1	±2	0,0223	±0,00010	2454	±14	2392	±46	1	±2	2330	±46	-380
FN2-20	**20**	6588	± 15	11520	± 232	222	±5	-4	±2	0,0236	±0,00008	2610	±10	2559	±37	-4	±2	2497	±37	-547
FN2-27	**27**	8524	± 23	1698	± 35	1918	±39	-5	±2	0,0232	±0,00008	2571	±10	2565	±11	-5	±2	2503	±11	-553
FN2-3	**45**	4895	± 20	6182	± 126	338	±7	-2	±2	0,0259	±0,00010	2867	±18	2830	±32	-2	±2	2768	±32	-818
FN2-52	**52**	9454	± 30	3965	± 80	1041	±21	-11	±2	0,0265	±0,00010	2960	±13	2948	±16	-11	±2	2886	±16	-936
FN2-74	**74**	16129	± 50	3438	± 70	2131	±43	-6	±2	0,0275	±0,00009	3065	±12	3059	±13	-6	±2	2997	±13	-1047
FN2-6	**90**	21367	± 213	2993	± 17	3410	±23	-11	±6	0,0289	±0,00031	3242	±40	3238	±40	-11	±6	3176	±40	-1226

*$\delta^{234}U = ([^{234}U/^{238}U]_{activity} - 1)x1000$. ** $\delta^{234}U_{initial}$ was calculated based on ^{230}Th age (T), i.e., $\delta^{234}U_{initial} = \delta^{234}U_{measured} \times e^{\lambda 234 \times T}$. Corrected ^{230}Th ages assume the initial $^{230}Th/^{232}Th$ atomic ratio of 4.4 ±2.2 x10^{-6}. Those are the values for a material at secular equilibrium, with the bulk earth $^{232}Th/^{238}U$ value of 3.8. The errors are arbitrarily assumed to be 50%. ***B.P. stands for "Before Present" where the "Present" is defined as the year 1950 A.D.

Table S2 – Chronological results. U/Th results obtained from speleothem TRA5. *Data obtained by Cruz et al. (2009).

Sample Number	Depth (mm)	^{238}U (ppb)		^{232}Th (ppt)		^{230}Th / ^{232}Th (atomic x10^{-6})		$d^{234}U$* (measured)		^{230}Th / ^{238}U (activity)		^{230}Th Age (yr) (uncorrected)		^{230}Th Age (yr) (corrected)		$d^{234}U_{Initial}$** (corrected)		^{230}Th Age (yr BP)*** (corrected)		Age BCE/CE
TRA5 speleothem																				
TRA5_2	**7**	1411	± 2	3788	± 76	6	±1	-145	±2	0,0009	±0,00009	119	±12	27	±66	-145	±2	-42	±66	1992
TRA5-18	**18**	2035	± 4	76686	± 1543	5	±0	-139	±2	0,0121	±0,00019	1541	±25	259	±907	-139	±2	197	±907	1753
TRA5_20	**20**	1915	± 4	20400	± 410	6	±0	-145	±2	0,0036	±0,00010	463	±12	100	±257	-145	±2	31	±257	1919
TRA5b-37	**37**	1977	± 2	612	± 13	89	±8	-139	±1	0,0017	±0,00014	211	±18	200	±19	-139	±1	130	±19	1820
TRA5-41	**41**	1889	± 5	2858	± 58	25	±1	-138	±2	0,0023	±0,00008	291	±10	240	±38	-138	±2	178	±38	1772
TRA5-58	**58**	1921	± 3	585	± 12	122	±4	-142	±2	0,0022	±0,00006	286	±7	276	±10	-142	±2	214	±10	1736
TRA8-71	**71**	2371	± 14	5165	± 108	21	±1	-147	±5	0,0028	±0,00012	356	±16	282	±55	-147	±5	213	±55	1737
TRA5b-90	**90**	2031	± 2	256	± 6	413	±18	-139	±1	0,0032	±0,00011	401	±14	396	±15	-139	±1	326	±15	1624
TRA8-104	**104**	2018	± 14	7328	± 155	22	±1	-141	±6	0,0049	±0,00023	618	±29	495	±92	-141	±6	426	±92	1524
TRA5-116	**116**	1785	± 4	912	± 18	124	±4	-139	±2	0,0038	±0,00008	488	±10	471	±16	-139	±2	409	±16	1541
TRA5-132	**132**	2699	± 5	1549	± 31	118	±3	-140	±2	0,0041	±0,00006	522	±8	503	±16	-140	±2	441	±16	1509
TRA5b-169	**169**	1969	± 2	108	± 5	1237	±73	-136	±1	0,0041	±0,00015	519	±19	517	±19	-136	±1	447	±19	1503

*$\delta^{234}U = ([^{234}U/^{238}U]_{activity} - 1)$x1000. ** $\delta^{234}U_{initial}$ was calculated based on ^{230}Th age (T), i.e., $\delta^{234}U_{initial} = \delta^{234}U_{measured}$ x $e^{\lambda 234 x T}$. Corrected ^{230}Th ages assume the initial $^{230}Th/^{232}Th$ atomic ratio of 4.4 ±2.2 x10^{-6}. Those are the values for a material at secular equilibrium, with the bulk earth $^{232}Th/^{238}U$ value of 3.8. The errors are arbitrarily assumed to be 50%. ***B.P. stands for “Before Present” where the “Present” is defined as the year 1950 A.D.

Table S3 – Speleothem intervals according to texture and mineral weight proportion (wt). Texture description: A - crystals with mosaic and columnar fabrics; B - interbedded needle-like crystals. *Obtained by Utida et al. (2020).

Speleothem Mineralogy					
Sample	Interval (mm)	Age (yr BCE/CE)	Texture	Aragonite (wt %)	Calcite (wt %)
TRA5	30-54	1855 to 1745 CE	A	0.0	**100.0**
	54-87	1745 to 1640 CE	A	0.0	**100.0**
	87-108	1640 to 1565 CE	A	0.0	**100.0**
	108-178	1565 to 1490 CE	A	0.0	**100.0**
TRA7*	0-173	1940 CE to 130 BCE	A	0.0	**100.0**
	173-215	130 to 290 BCE	B	**99.0**	1.0
	215-270	290 to 3000 BCE	B	**87.1**	12.9
FN1*	0-27	1790 to 1170 CE	B	**85.2**	14.9
	27-83	1170 to 610 CE	B	**90.6**	9.4
	83-128	610 to 80 CE	A	0.0	**100.0**
	128-202	80 CE to 1730 BCE	B	**94.5**	5.5
FN2	6-31	189 to 660 BCE	B	**94.7**	5.3
	31-56	660 to 960 BCE	B	**94.8**	5.2
	56-63	960 to 1,005 BCE	B	**94.8**	5.2
	63-95	1,005 to 1,265 BCE	B	**93.4**	6.6

Table S4 – Parameters used to establish the composite record of Trapiá and Furna Nova stalagmites with *iscam* programming (Fohlmeister, 2012)

Parameter	Range	Description
nrAR1	2000	Number of AR1 simulations
nrAR1_MC	1000	Number of MC runs for each AR1
nrMC	100000	Number of MC simulations for measured data sets
nrSMOOTH	10	Number of years used for smoothing before the correlation
CUT	1	Extrapolation of isotope data allowed beyond dated depths
GAUSS	0	MC simulations with Gaussian distribution
Interpol	-1	Pointwise linear interpolation between dated depths
Detrend	2	Detrending and normalizing before running the method

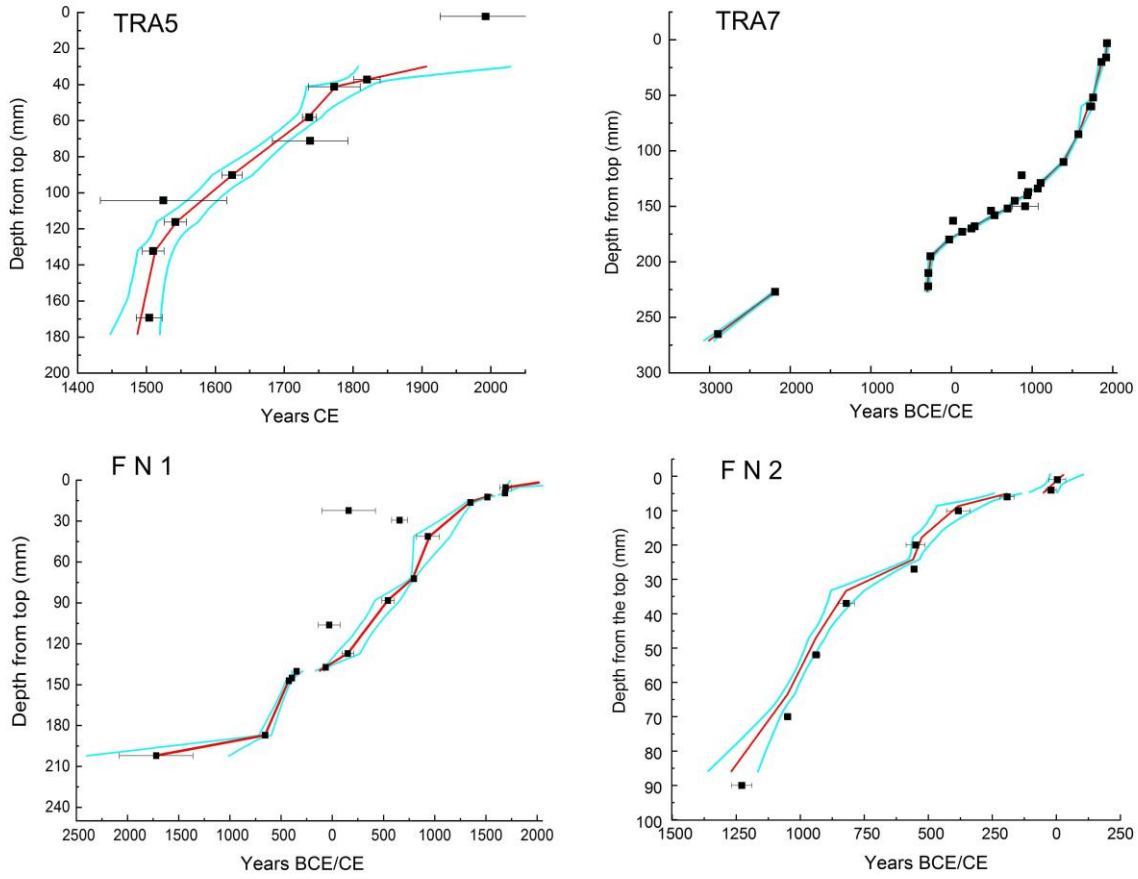

Figure S4 – Age models of speleothems from Rio Grande do Norte. Age models were calculated using COPRA (Breitenbach et al., 2012) through a set of 2,000 Monte Carlo simulations. The COPRA age model was produced for each sample and covers the entire stalagmite. Squares: age results and error bars. Red line: COPRA average age model. Cyan line: *iscam* age model errors considering 95% confidence interval.

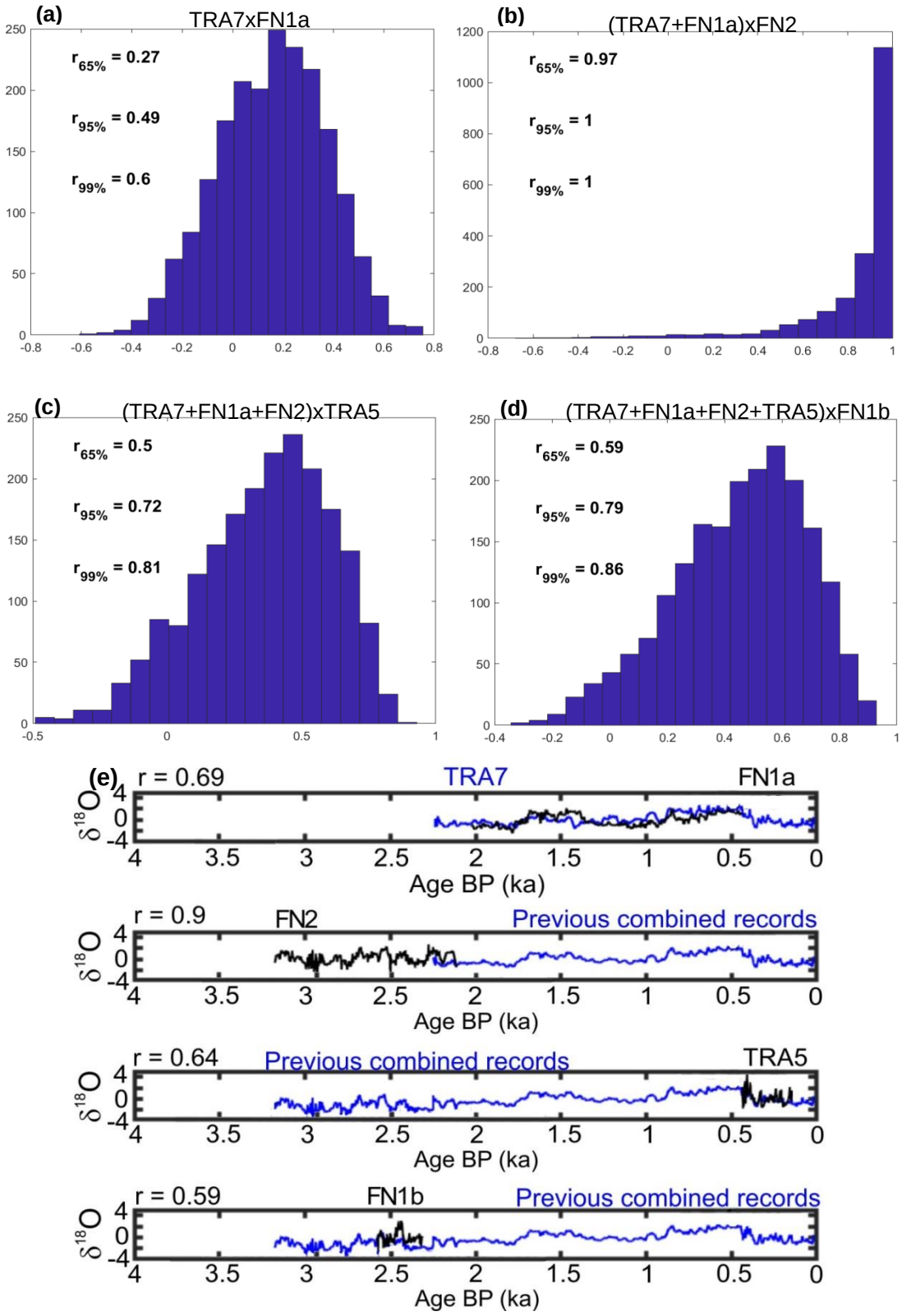

Figure S5 – Distribution of maximum correlation coefficients for 2000 pairs of AR1 time series with the same characteristics as the measured $\delta^{18}O$ stalagmite time series. a) distribution for TRA7 and FN1a; b) distribution for TRA7+FN1a and FN2; c) distribution for TRA7+FN1a+FN2 and TRA5; d) distribution for TRA7+FN1a+FN2+TRA5 and FN1b. e) Best time series results for the individual steps *iscam* performs for the composite time series construction. Highest correlation coefficient is indicated for each correlation step. All established time series are significant at the 95% confidence limit.

References

Araújo, R.G., Andreoli, R.V., Candido, L.A., Kayano, M.T., de Souza, R.A.F., 2013. Influence of El Niño-Southern Oscillation and Equatorial Atlantic on rainfall over northern and northeastern regions of South America. Acta Amaz. 43 (4), 469-480. https://doi.org/10.1590/S0044-59672013000400009.

Breitenbach, S.F.M., Rehfeld, K., Goswami, B., Baldini, J.U.L., Ridley, H. E., Kennett, D. J., Prufer, K.M., Aquino, V.V., Asmerom, Y., Polyak, V.J., Cheng, H., Kurths, J., Marwan, N., 2012. COnstructing Proxy Records from Age models (COPRA). Clim. Past 8, 1765–1779. https://doi.org/10.5194/cp-8-1765-2012.

Cruz, F.W., Vuille, M., Burns, S.J., Wang. X., Cheng, H., Werner, M., Edwards, R.L., Karman, I., Auler, A.S., Nguyen, H., 2009. Orbitally driven east-west antiphasing of South American precipitation. Nat. Geosci. 2, 210-214. https://doi.org/10.1038/ngeo444.

Fohlmeister, J., 2012. A statistical approach to construct composite climate records of dated archives. Quat. Geochronol. 14, 48-56. https://doi.org/10.1016/j.quageo.2012.06.007.

Utida, G., Cruz, F.W., Santos., R.V., Sawakuchi, A.O., Wang, H., Pessenda, L.C.R., Novello, V.F., Vuille, M., Strauss, A.M., Borella, A.C., Stríkis, N.M., Guedes, C.C.F., De Andrade, F.D., Zhang., H., Cheng, H., Edwards, R.L., 2020. Climate changes in Northeastern Brazil from deglacial to Meghalayan periods and related environmental impacts. Quat. Sci. Rev. 250, 106655. https://doi.org/10.1016/j.quascirev.2020.106655.